Junji Sone
e-mail: sone@cs.t-kougei.ac.jp

Ryou Inoue

Katsumi Yamada

Takanori Nagae

Faculty of Engineering,
Tokyo Polytechnic University,
1583 Iiyama, Atsugi,
Kanagawa 243-0297, Japan

Kinya Fujita
Graduate School,
Tokyo University of Agriculture and Technology,
2-24-16 Naka-cho, Koganei-shi,
Tokyo 184-8588, Japan

Makoto Sato
Precision and Intelligence Laboratory,
Tokyo Institute of Technology,
4259 Nagatsuta-cho, Midori-ku, Yokohama,
Kanagawa 226-8503, Japan

Development of a Wearable Exoskeleton Haptic Interface Device

We developed a wearable exoskeleton haptic interface to fit the human body. We generated a force constituting a contrasting moment by pulling a wire using a dc motor. We also developed a control system, which included a motor controller, an interface, and a control software. We evaluated the performance of our interface by conducting a simple task experiment. To execute one task, the control data for each joint jaw must be prepared, and we used force control data generated by a rectified and filtered electromyogram (EMG) curve. From the force representation experiments, it was determined that a force curve based on the EMG data could be used for a haptic interface, and we confirmed that a suitable force curve could be obtained for each subject.
[DOI: 10.1115/1.3009670]

Keywords: haptic display, wearable, exoskeleton, force curve, EMG

1 Introduction

Haptic information is important for interactive manipulation of virtual objects and in enhancing the presence of virtual environments. A number of haptic interface devices [1], which exhibit reaction force or tactile sense by touching objects, have been studied. Grounded-type haptic devices, such as PHANToM [2], SPIDAR [3], and Haptic Master [4], have also been applied in numerous types of virtual reality systems. However, these devices are required to be fixed within their environment, e.g., the floor, and the working space is limited by the structure.

To improve system portability, nongrounded or body-grounded devices [5] have also been developed. GyroCube [6] is a nongrounded force-feedback device that utilizes a gyromoment for force generation. Electric motors are controlled to generate the gyromoment.

Another nongrounded force-feedback device utilizes angular momentum generated by the mechanical braking of a rotating wheel [7]. Amemiya et al. [8] also developed a force-feedback device with a linearly reciprocating mass that was driven at different velocities depending on the traveling direction. Because of this nonlinearity of the force perception property, the user perceives pseudoforces. The nongrounded force-feedback devices have the advantage of not having to be in a fixed position; however, there is a trade-off between the representative forces and the device weight.

Wearable haptic displays that set the force-acting point on the body were developed. One had a wearable joystick [9] allowing the user to set up the acting point from their forearm, while the other variant was the HapticGear [5], in which the actuator was at the back of the user.

Forces were transferred to the finger through a string, which was actuated by a motor. To realize the wide range of haptic area, we selected a wearable haptic display that set force-acting points on the body. However, problems arose when the actuators were placed at the back, and force was transferred to the finger through the string.

Interference between wires and the human body occurred. Therefore, much research has to be done on exoskeleton-type haptic displays [10–13] in which the outer frames fit the body, and joint jaw moments are generated by the haptic interface.

The selection of the exoskeleton type [14,15] to fit the joint jaw depends on the angle of the joint. Therefore, if a different angle is selected, the generated force might differ from the target force value.

The central nervous system assigns motion commands, and the muscles contract in certain human operations. Joint jaw movements are generated by joint jaw moments, which are caused by the contraction of the muscles [16,17]. The contraction response has either a first or second order delay system. It is well known that rectifying and filtering electromyogram (EMG) data correlate to the power of muscular contractions [18].

Therefore, a rectified and filtered EMG curve can be used for force exceptions of antagonism between two forces that are generated by activating the extensor and the flexor muscles at the same time.

Therefore, we realized that a force representation method could be used in which the torque of each joint jaw could be controlled by EMG signals. This idea is based on our confirmation that contraction force is almost proportional to the amplitude of EMG signals within a specific range. In this case, the activation pattern of each muscle is dependent on the task; therefore, we needed to prepare force data (look-up tables) for each joint jaw and each task and confirm the control method for each task and each human.

We can infer the task from the position and relationship between the human body and the operating object for the realization of the haptic display in a virtual world. Motion databases have been investigated in the field of computer graphics [19,20]. We

Contributed by the Engineering Simulation and Visualization Committee for publication in the JOURNAL OF COMPUTING AND INFORMATION SCIENCE IN ENGINEERING. Manuscript received September 1, 2007; revised manuscript received October 6, 2008; published online November 26, 2008. Review conducted by J. Oliver, M. Omalley, and K. Kesavadas.

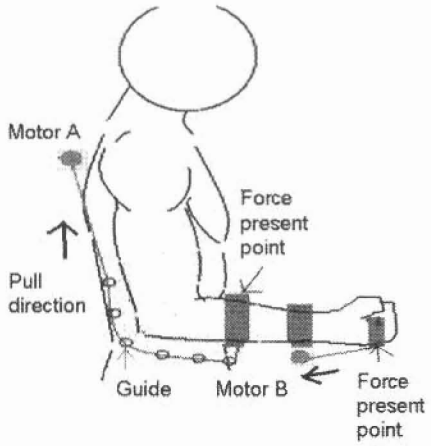

Fig. 1 Force representation method scheme

can also infer the appropriate task from the position of the acting part, such as the hand, and the operating object based on the motion database. From this task estimation, loads can be calculated by physical simulations and representing forces can be determined from the force curves (look-up tables) for each task and force intensity.

In this study, we considered the construction of a force control method using force curves (look-up tables) for each joint jaw for one task. Our method is similar to the event-based haptic rendering method [21].

The database based approach is an available method in applications such as video games, where fast computations are required and the set of user actions is limited. Therefore, we developed a wearable exoskeleton haptic interface to fit the human body. We confirmed the performance of our interface with a simple action experiment, in which the interface used a force curve generated by human EMG data. Our target actions were a complex assembly of parts set in an engine room dynamically changing actions similar to Judo and dance movements.

2 Haptic Interface

2.1 Force Representation Method. Figure 1 shows the scheme of the force representation method employed in this study. Representing force constitutes contrast moment generated by pulling a wire. This moment is equal to the moment at the joint jaw, which is caused by muscle contraction.

Figure 1 shows the force representation scheme for a cubital joint. The actuator motor is set at shoulder level, and the lower arm is pulled by a wire. Guide rings are set around and under the elbow in such a way that they do not come in contact with the elbow and the wire. This is done to maintain a constant moment and cubital joint angle.

In this study, the motor and force-acting points are installed at appropriate points and the length of string is adjusted automatically by a very weak voltage applied to the motor. Thus, a complex design for the force transfer mechanism is not needed.

Subsequently, we decided how the ice hockey protector could be fixed to the motor, designed the motor fixture parts, and considered a method for attaching the string to the force-acting point.

2.2 Development System. Figure 2 shows the entire haptic interface system. The bobbin is installed at the axis of the dc motor, and tension is generated by the winding bobbin. Motor A represents the force applied at the biceps brachii muscle. The force application point of the lower arm is one side of the biceps brachii muscles. This is the point where the tendon attaches to the bone.

Motor A is placed at the shoulder level to avoid any movements of the motor during any actions. Motor B generates the extension

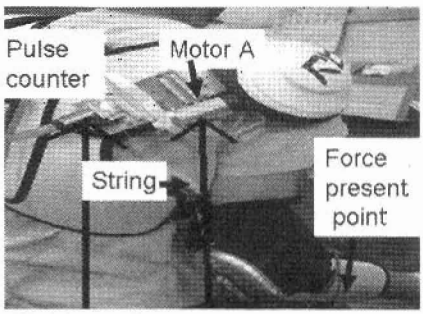

Fig. 2 Mechanism of haptic interface

moment at the wrist joint, and this represents the force to the palmaris longus muscle. A pulse counter and a wire were set up separately with the force representation motor to obtain the accurate angle of the joint jaw. The jaw joint moment is controlled by the numbers on the pulse counter. Similarly, the force representation motor and pulse counter are set at the back of the lower arm to represent the force to the palmaris longus muscle. Both the motor and the pulse counter are fixed with a band on the lower arm.

Figure 3 shows the system construction. The motor torque is controlled by the motor driver, a D/A converter, and a personal computer. The joint jaw angle is measured by the pulse counter, and the motor torque is controlled using a look-up table, which corresponds to the joint jaw angle. A preliminary look-up table is built for each jaw joint angle. The particular building method is described in the next section. The control program is developed in the C++ language.

The EMG sensor data are obtained using an amplifier, a filter, and an A/D converter attached to a personal computer, which this EMG sensor only uses on the confirmation experiment, and we use a look-up table for haptic representation.

2.3 Coalition Method With Physical Simulation. In a virtual environment, when calculating external force by physical simulations, the task and the internal force for each joint jaw can be chosen from the force data (look-up tables) for the corresponding task.

The strength of the internal force can be adjusted by the external force. Force representation can be obtained by these internal forces for each joint jaw, and the measurement angle for each joint jaw is transferred from the motor encoder data. In this case, we believe that it is effective to use a motion database to specify the task. In our method, we require a look-up table for each joint jaw and each task.

We confirmed a 28% load reduction case. The results showed a 26% reduction in peak amplitude of the measured EMG signal

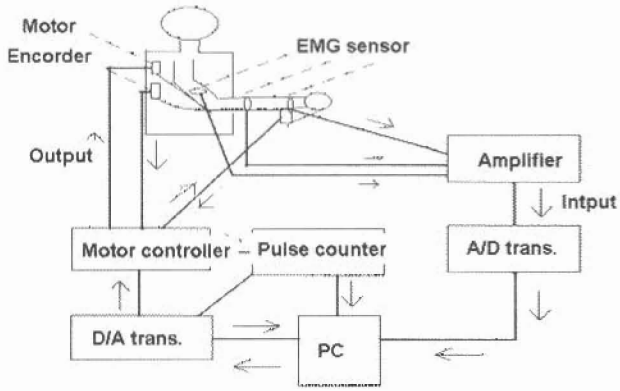

Fig. 3 System construction

curve, and the data had a similar curve shape. Therefore, our method using a look-up table can be suitable for varying loads. In the future, we will develop a method for the automatic acquisition of look-up tables.

3 Verification Method

3.1 Composition of the Target Force Curve. The simple action of lifting some weights was used in our verification experiment. Figures 4–6 show the upper force applied by the biceps brachii muscle EMG and palmaris longus muscle EMG for the pull-up action with a 2 kg weight. The force sensor was placed in a fixed position for this experiment. Initially, no force is applied;

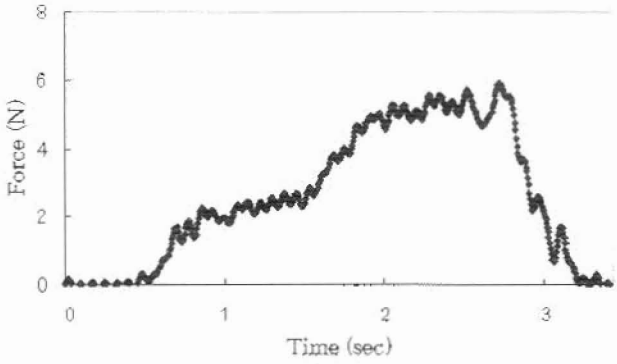

Fig. 4 Upper direction force for pull-up action

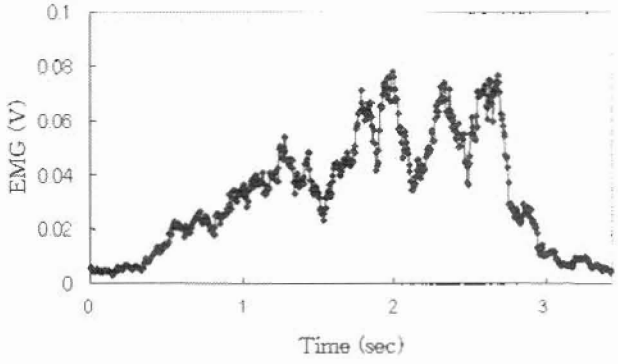

Fig. 5 EMG of biceps brachii for pull-up action

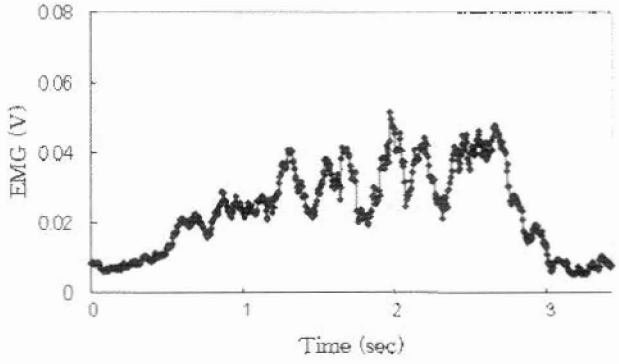

Fig. 6 EMG of palmaris longus for pull-up action

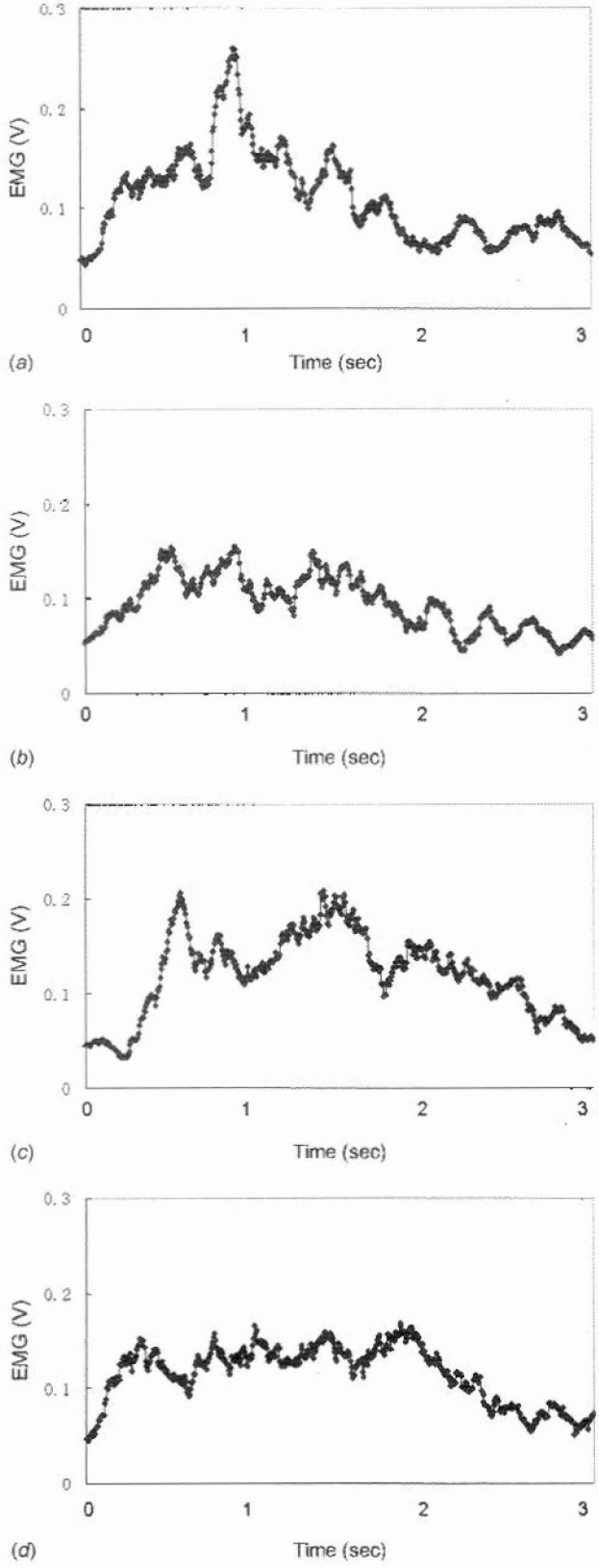

Fig. 7 Biceps brachii force pattern of pull-up action. (*a*) Biceps brachii force pattern 1 (subject A), (*b*) biceps brachii force pattern 2 (subject A), (*c*) biceps brachii force pattern 3 (subject B), and (*d*) biceps brachii force pattern 4 (subject B).

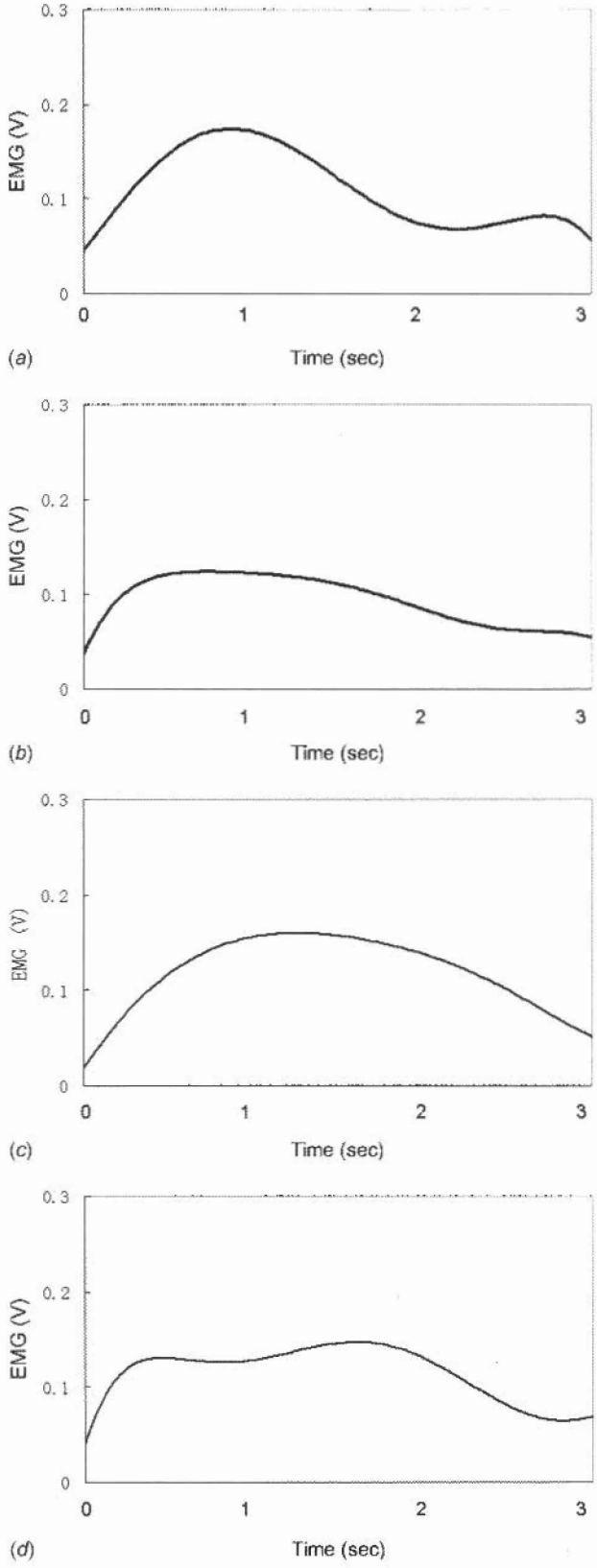

Fig. 8 Biceps brachii force pattern of pull-up action (approximation). (*a*) Biceps brachii force pattern 5 (subject A), (*b*) biceps brachii force pattern 6 (subject A), (*c*) biceps brachii force pattern 7 (subject B), and (*d*) biceps brachii force pattern 8 (subject B).

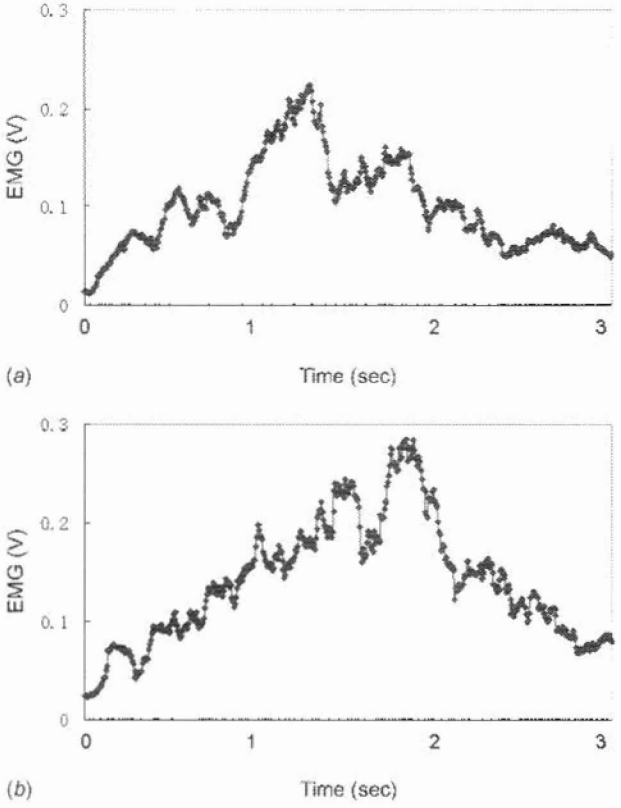

Fig. 9 Palmaris longus force pattern of pull-up action. (*a*) Palmaris longus force pattern 9 (subject A), and (*b*) palmaris longus force pattern 10 (subject B).

however, the force is gradually increased after 3 s. The results show that the activation patterns of force, biceps brachii muscle EMG, and palmaris longus muscle EMG are not in perfect accordance.

One method is calculated using physical simulation to represent the force, but there is uncertainty in determining each joint jaw moment. Therefore, the EMG data of each muscle of an examinee are measured by actual actions, and the resulting activation patterns are derived from the EMG curves. In this experiment, all actions must be natural movements.

We used surface EMG measurement instruments, such as a sensor (EMG-21), an amplifier (EMG025), and dc power supply (BB-04) (manufactured by HARADA Electric Inc.).

Here, for measuring the biceps brachii muscle EMG, the lower arm was raised gradually while the wrist was held in a fixed position. For the palmaris longus muscle, the position of the hand was lifted gradually while the lower arm remained in a fixed position.

The sampling time was set to 5 ms, and the data were rectified and integrated every 100 ms. Approximation curves are also computed by polynomial approximation. Irregularity of the integration or filtering operations lead to unstable control of force representation, and we thus used the polynomial approximation. We need to avoid the noise and extract detail characteristic of the data. Then, a six degree polynomial is used for the least-square fitting method.

3.2 Result of the Target Force Value. The subjects were males between 21 and 24 years old. All were engineering students, and they were novices to this system. We selected two subjects, whose body fat percentage was almost 10%, because it is easier to measure their EMG compared with subjects that have a greater body fat percentage.

EMG data were corrected for the subject's dominant arm. Force

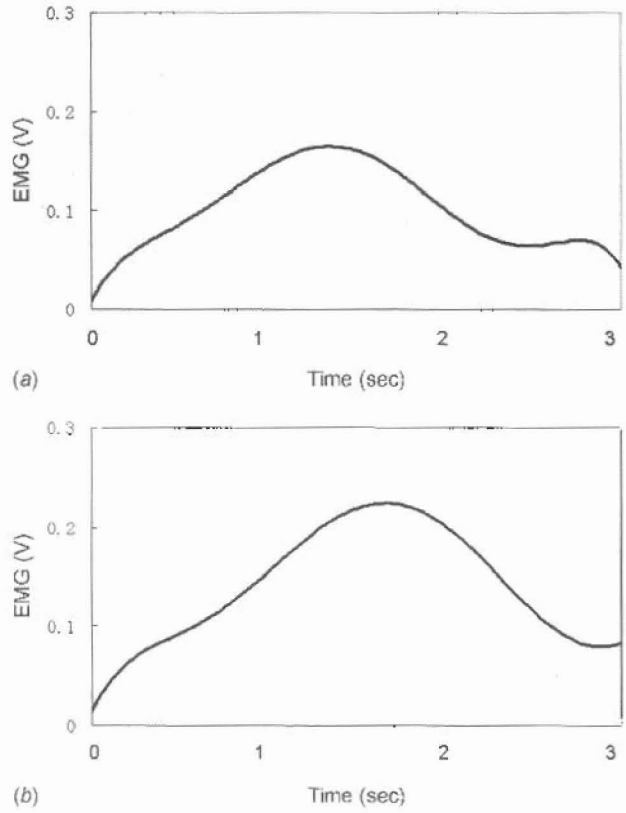

Fig. 10 Palmaris longus force pattern of pull-up action (approximation). (*a*) Palmaris longus force pattern 11 (subject A), and (*b*) palmaris longus force pattern 12 (subject B).

curves for the biceps brachii and palmaris longus muscles are then selected from EMG measurement data. The data are rectified and integrated at 100 ms.

There are two data shape patterns—one has a single convex shape, while the other has two. We selected four types of typical biceps brachii and two types of typical palmaris longus muscle force curves; subsequently, we generated approximation data for each curve using the sixth degree polynomial method.

Figures 7(*a*) and 7(*b*) show the typical biceps brachii muscle force curves for subject A. Figures 7(*c*) and 7(*d*) show the typical biceps brachii muscle force curves for subject B. The typical biceps brachii muscle force curves are selected for this study because they are the most popular pattern for measuring data. Figures 8(*a*)–8(*d*) are the approximation data of biceps brachii muscle force curves for Figs. 7(*a*)–7(*d*), respectively. Figure 9(*a*) shows the typical palmaris longus muscle force curve for subject A, Fig. 9(*b*) shows the typical palmaris longus muscle force curve for subject B. Figures 10(*c*) and 10(*d*) are the approximation data of palmaris longus muscle force curves for Fig. 9(*a*) and 9(*b*), respectively.

4 Verification Experiment

The verification experiment was executed using the pull-up action with both hands. One hand brought up the weight (actual action), and the force was transferred to the other hand by our haptic interface.

Here, the EMG of both hands for the biceps brachii and palmaris longus were measured, and we compared the EMG curves of the actual actions and force representations.

The experimental procedure was as follows:

(1) Haptic interface was set on the right hand.
(2) Subjects pulled up 1 kg weight by the left hand.
We deduced the weight by the maximum motor output force using the bobbin, which was approximately 9 N. It is difficult to get an obvious EMG curve because of the light load, and then experiment time was reduced from 3 s to 2 s for the force curve pattern selection measurements. Eight force curves of the biceps brachii and four force curves for the palmaris longus are used for the haptic interface force representation.

We used three lead time patterns (0 ms, 50 ms, and 100 ms) to compensate for the force delay of the muscle action. The condition number was set using a combination of a variety of force curves and lead times.

(3) Calibration between the joint jaw angle and the pulse value of the encoder was executed for each subject.

We performed four experiments for each condition and conducted a questionnaire survey and measured the EMG data for each experiment.

(4) We executed this experiment in a step-by-step process.

First, the optimal conditions were determined for force representations of the biceps brachii. Second, we performed the experiment with force representations of the biceps brachii and palmaris longus and decided the optimal condition of two force representations.

In these processes, we verified the haptic interface through an evaluation of the questionnaire results and a comparison between the EMG curves of the haptic interface and the actual actions of five subjects having body fat percentage of approximately 10%.

The subjects were 21–24 year old males. All were engineering students and novice to this system. Force representation was performed for the subject's dominant arm, and actual action was executed with the nondominant hand.

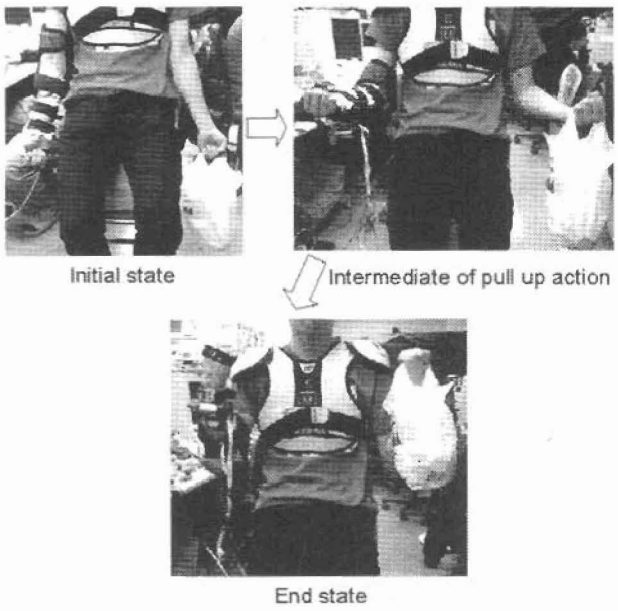

Fig. 11 Outline procedure of experiments

The questionnaire items were as follows:

(1) Was the sense of the haptic interface's force recognizable?

5: perfectly recognized
4: almost perfectly recognized
3: not entirely recognized
2: difficult to recognize
1: not recognized

(2) Was the timing of the force in sync?

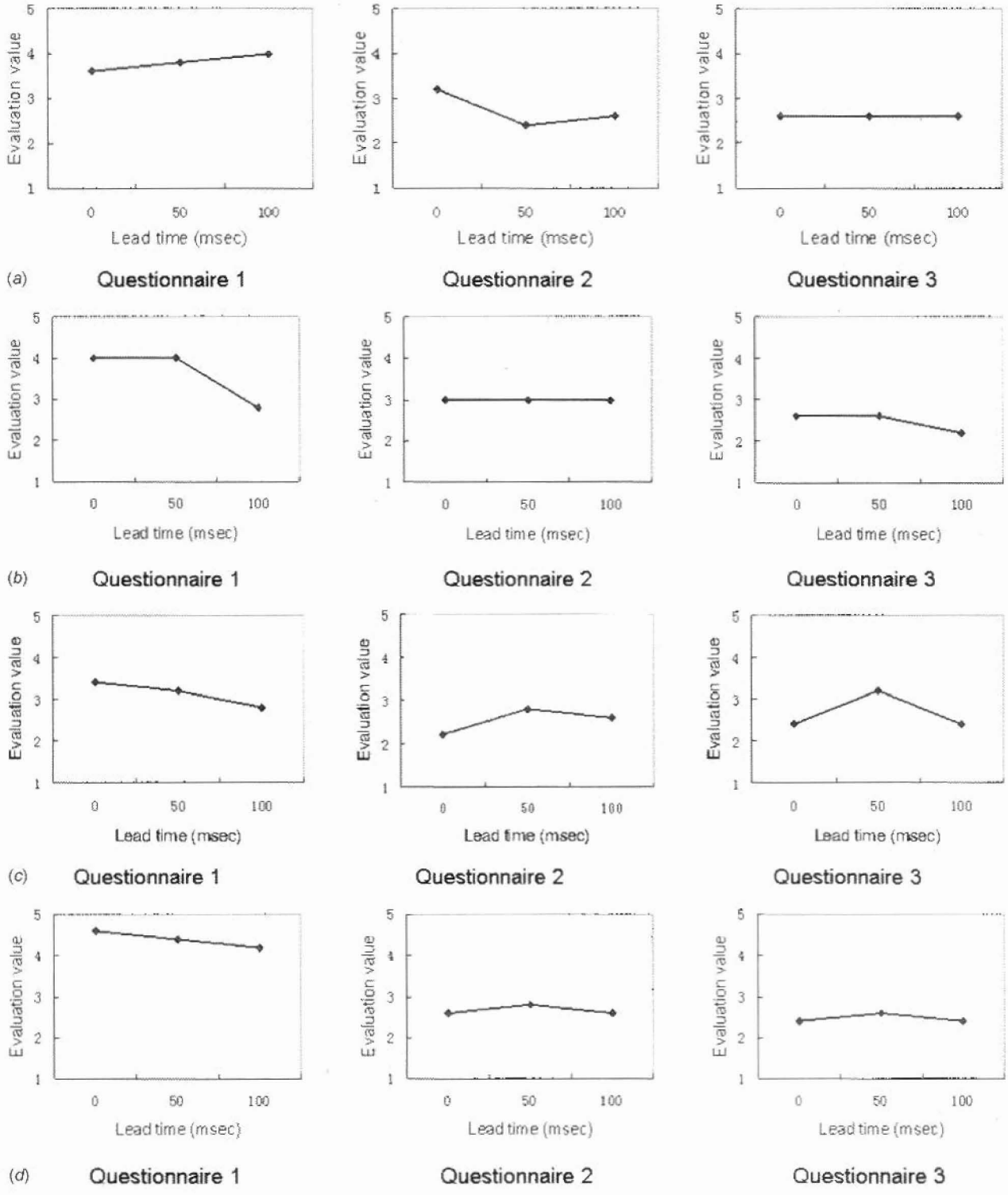

Fig. 12 Average effect of lead time for force patterns 1–4. (*a*) Average effect of lead time for force pattern 1, (*b*) average effect of lead time for force pattern 2, (*c*) average effect of lead time for force pattern 3, and (*d*) average effect of lead time for force pattern 4.

5: perfectly synchronized
4: almost perfectly synchronized
3: not entirely synchronized
2: poorly synchronized
1: not synchronized

(3) Was the sense of the haptic interface's force similar to actual action?

5: perfectly same
4: similar
3: little similarity
2: very little similarity
1: dissimilar

4.1 Force Representation Experiment for Biceps Brachii. Earlier, we verified the haptic interface for its force representation

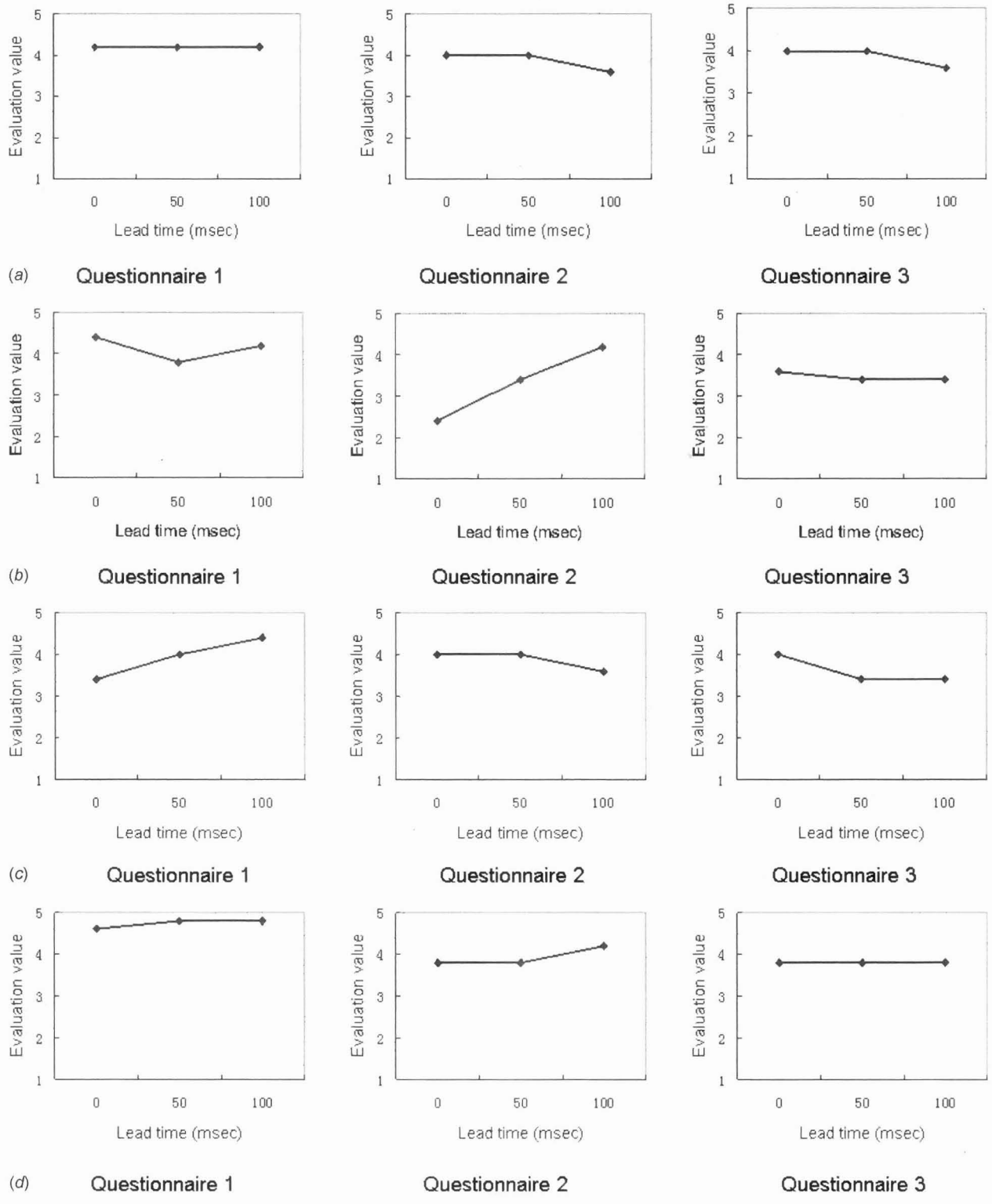

Fig. 13 Average effect of lead time for force patterns 5–8. (*a*) Average effect of lead time for force pattern 5, (*b*) average effect of lead time for force pattern 6, (*c*) average effect of lead time for force pattern 7, and (*d*) average effect of lead time for force pattern 8.

of biceps brachii. We used eight force curves (patterns 1–8) and three lead times (0 ms, 50 ms, and 100 ms). The experiments were repeated four times for each condition. Subjects were five persons. Figure 11 shows the outline of our experiments.

4.2 Result of Force Representation Experiment for the Biceps Brachii. Figures 12 and 13 show the average effect of each lead time for each questionnaire, which is computed by the sequential classification method. Patterns 5 and 8 show better results for all questionnaires. The average scores of questionnaire 1 were calculated to be 4.2; questionnaire 2, 3.8; and questionnaire 3, 3.8, respectively, for pattern 5. The average scores of questionnaire 1 were calculated to be 4.7; questionnaire 2, 4.0; and questionnaire 3, 3.8, respectively, for pattern 8. The lead times 0 ms and 50 ms

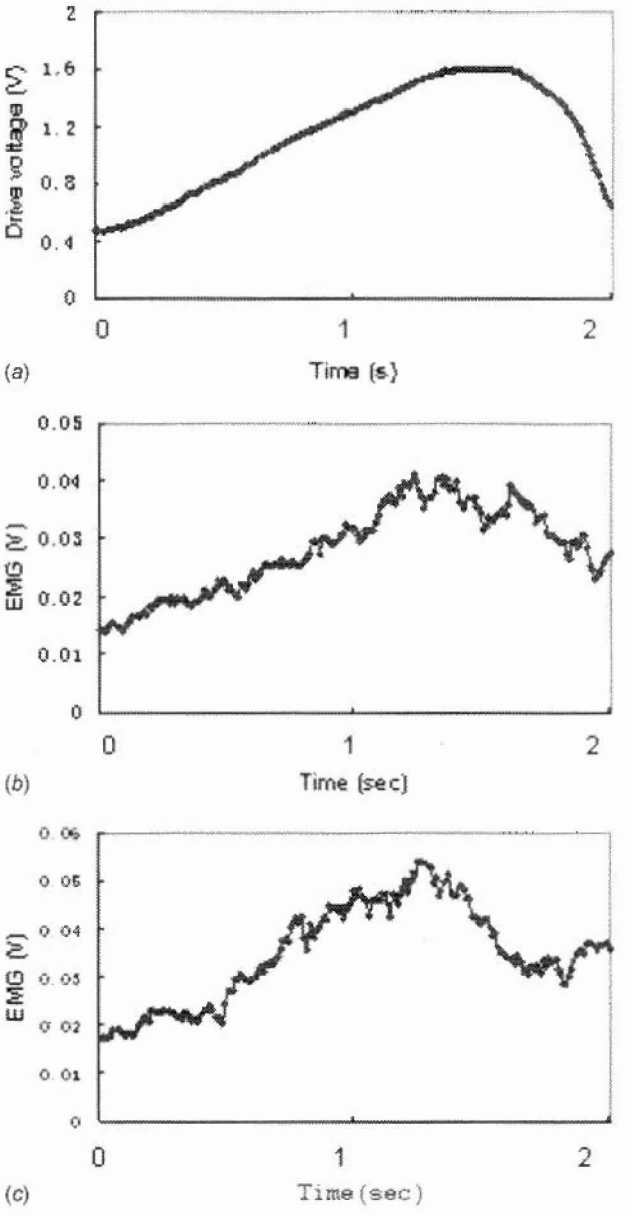

Fig. 14 (*a*) Motor driven voltage, (*b*) EMG data of haptic interface, and (*c*) EMG data of actual action

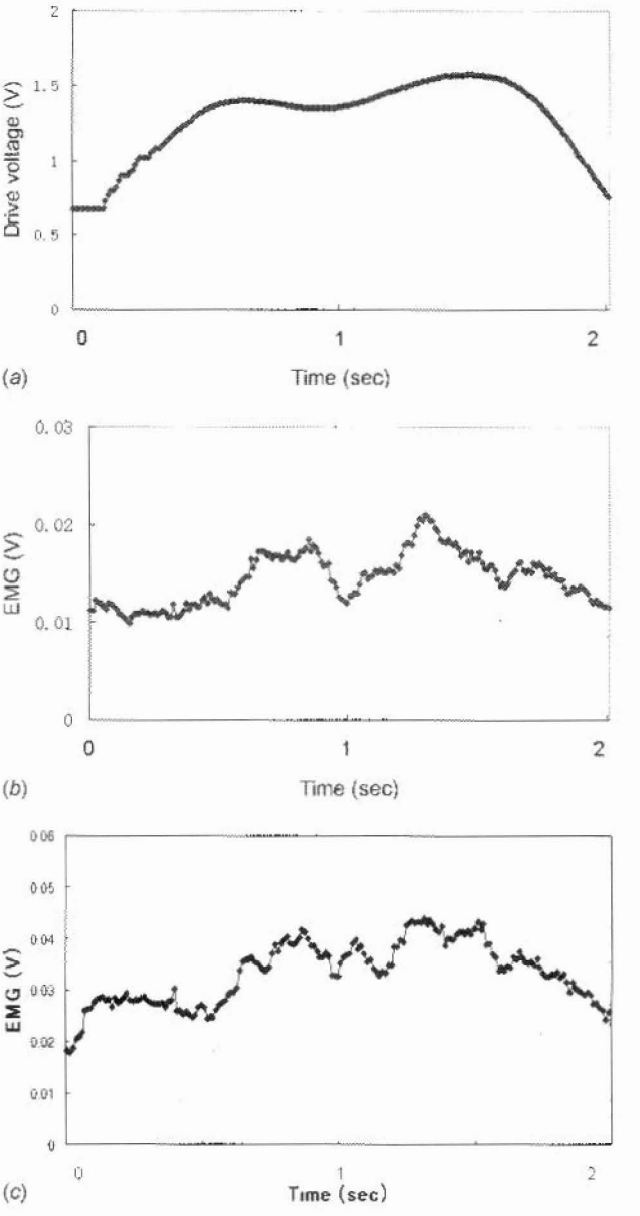

Fig. 15 Motor driven voltage, EMG data of haptic and actual action for pattern 8, and lead time: 100 ms (subject B). (*a*) Motor driven voltage, (*b*) EMG data of haptic interface, and (*c*) EMG data of actual action.

showed a good score for pattern 5. Moreover, pattern 8 with a lead time of 100 ms showed a better score. In general, several approximate force curve patterns (5–8) were better than some nonapproximate patterns (1–4).

In particular, patterns 5 and 8 are better force curves for haptic interfaces, the favor of the two patterns are different depending on the subject. We used lead time to compensate for delays in the reaction. The lead time required differed for each pattern.

Figure 14(*a*) shows the representation motor driven voltage for force curve pattern 5. This voltage is the input of the motor amplifier. Wire force is 9 N at 1.8 V for the motor amplifier. Figure 14(*b*) shows the EMG data of the biceps brachii for Fig. 14(*a*) force representation. Figure 14(*c*) shows the actual action EMG data of the biceps brachii. Three figures were of a similar pattern. Figure 15(*a*) shows the representation motor driven voltage for force curve pattern 8. Figure 15(*b*) shows the EMG data of the biceps brachii for Fig. 15(*a*) force representation. Figure 15(*c*) shows the actual action EMG data of the biceps brachii. Three figures were of a similar pattern.

Table 1 shows the correlation coefficients (CCs) of EMG data between the haptic interface and the actual action for patterns 5 and 8. These coefficients exceed 0.5, showing a good correlation; pattern 3 data are negative. We selected force curve patterns 5 and 8 from the results of the questionnaires and the EMG data.

4.3 Force Representation Experiment for the Biceps Brachii and Palmaris Longus. We used approximation force curve pattern 11 (Fig. 10(*c*)) for palmaris longus in the preliminary experiment. The verification experiment of force representa-

Table 1 Correlation coefficient of the EMG data between the haptic interface and the actual action for pattern 5 and pattern 8

Pattern	Correlation coefficient
5	0.85
8	0.75

tion for both the biceps brachii and the palmaris longus was executed using force curve pattern 5, pattern 8 was used for biceps brachii, and pattern 11 for palmaris longus.

The condition number was set using a combination of pattern 5, pattern 8, and three lead times. Pattern 11 was the common condition. Forces are applied to the biceps brachii and palmaris longus by the haptic interface, which was set on the right hand, and a 1 kg weight held to the left hand.

The pull-up action was performed by both hands. In this experiment, motor driven voltages for force representing the biceps brachii, EMG of right biceps brachii, EMG of left biceps brachii, motor driven voltages for force representing the palmaris longus, EMG of right palmaris longus, and EMG of left palmaris longus were recorded. Three questionnaires were conducted at the same time. Subjects repeated the actions four times for each condition.

4.4 Results of Force Representation Experiment for Biceps Brachii and Palmaris Longus. Figures 16 and 17 show the average effect of each lead time for each questionnaire, which is computed by the sequential classification method. The average scores of questionnaire 1 were calculated to be 4.6; questionnaire 2, 2.4; and questionnaire 3, 3.4, respectively, for pattern 5. The average scores of questionnaire 1 were calculated to be 4.8; questionnaire 2, 3.5; and questionnaire 3, 3.4, respectively, for pattern 8. The lead time 50 ms showed a good score for pattern 5. Moreover, pattern 8 with a lead time of 0 ms showed a better score.

Figure 18(a) shows the representative motor driven voltages of the biceps brachii for the force curve pattern 5. Figures 18(b) and 18(c) show the EMG data of the biceps brachii for Fig. 18(a) force representation and actual actions.

Figure 19(a) shows the representative motor driven voltages of palmaris longus for force curve pattern 11. Figures 19(b) and 19(c) show the EMG data of the palmaris longus for Fig. 19(a) force representation and actual actions. The patterns in Figs. 18(a)–18(c) are almost similar. In addition, Figs. 19(a)–19(c) had almost similar patterns.

Figure 20(a) shows the representative motor driven voltages of the biceps brachii for the force curve pattern 8. Figures 20(b) and 20(c) show the EMG data of the biceps brachii for Fig. 20(a) force representation and actual actions. Figure 21(a)shows the representative motor driven voltages of palmaris longus for force curve pattern 11.

Figures 20(b) and 21(c) show the EMG data of the palmaris longus for Fig. 21(a) force representation and actual actions. The patterns in Figs. 20(a)–20(c) are almost similar. In addition, Figs. 21(a)–21(c) had almost similar patterns.

Table 2 shows the correlation coefficients of EMG data between the haptic interface and the actual action for patterns 5 and 8. These coefficients exceed 0.5, showing a good correlation. From these experiments, we investigated the best force curve from the haptic interface for force-recognition, timing, and similar effects with actual actions.

5 Discussion

In this paper, we have studied a wearable exoskeleton haptic display that uses internal forces calculated from EMG signals obtained by performing the task of pulling up a 1 kg weight. From the experiment, a suitable force representation has been investigated using internal force curves. The appropriate force pattern depends on the individual.

In this study, patterns 5 and 8 suited the subjects. We used lead time to compensate for delays in reactions; however, the suitable lead time differs for each pattern. For future applications, we need to verify whether this control method can be effective for the same task with a slightly different angle for each joint jaw, using the same look-up table. Furthermore, as the acceleration and velocity of the target action vary, we need to consider a scaling factor to compensate the look-up table.

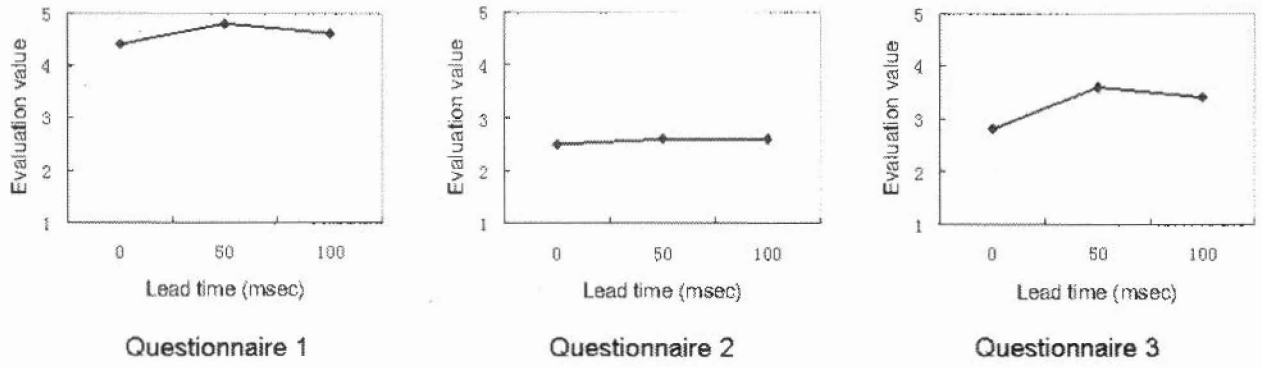

Fig. 16 Average effect of lead time for force patterns 5 and 11

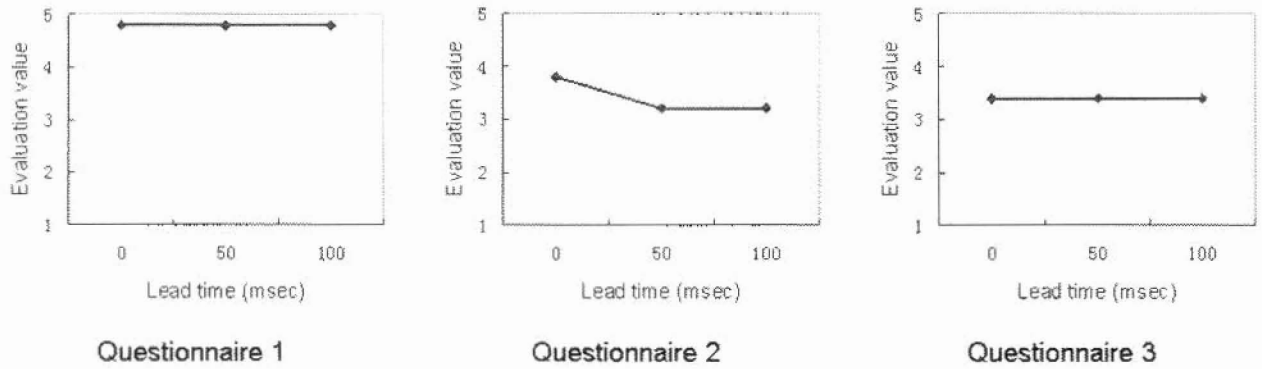

Fig. 17 Average effect of lead time for force patterns 8 and 11

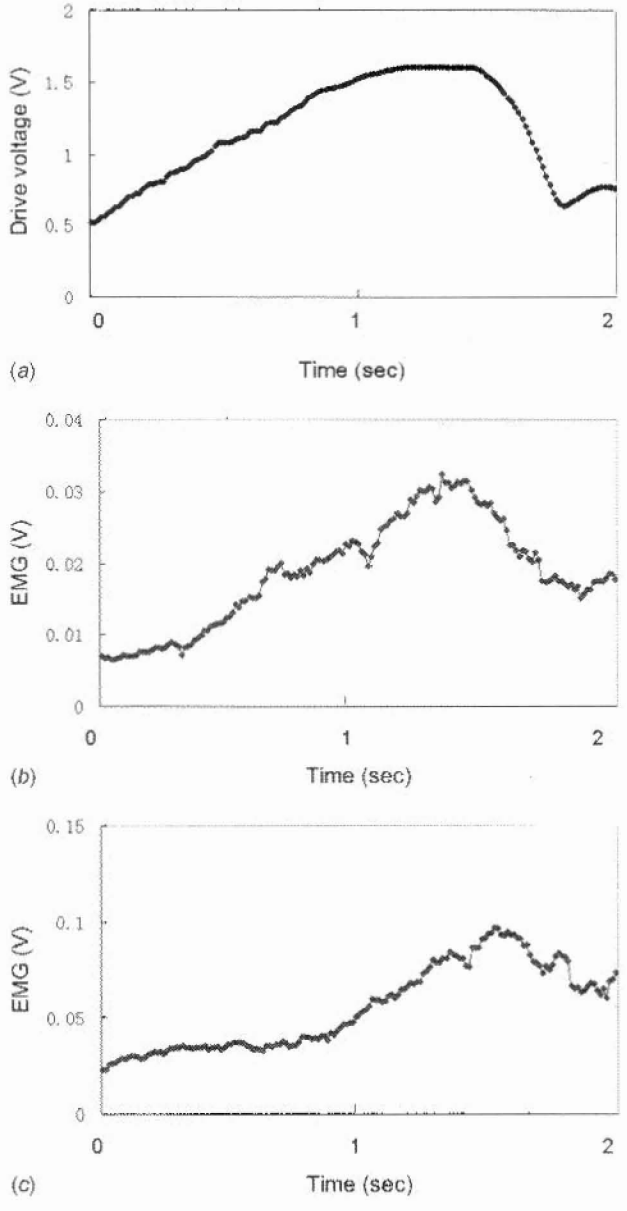

Fig. 18 (*a*) **Motor driven voltage,** (*b*) **EMG data of haptic interface, and** (*c*) **EMG data of actual action**

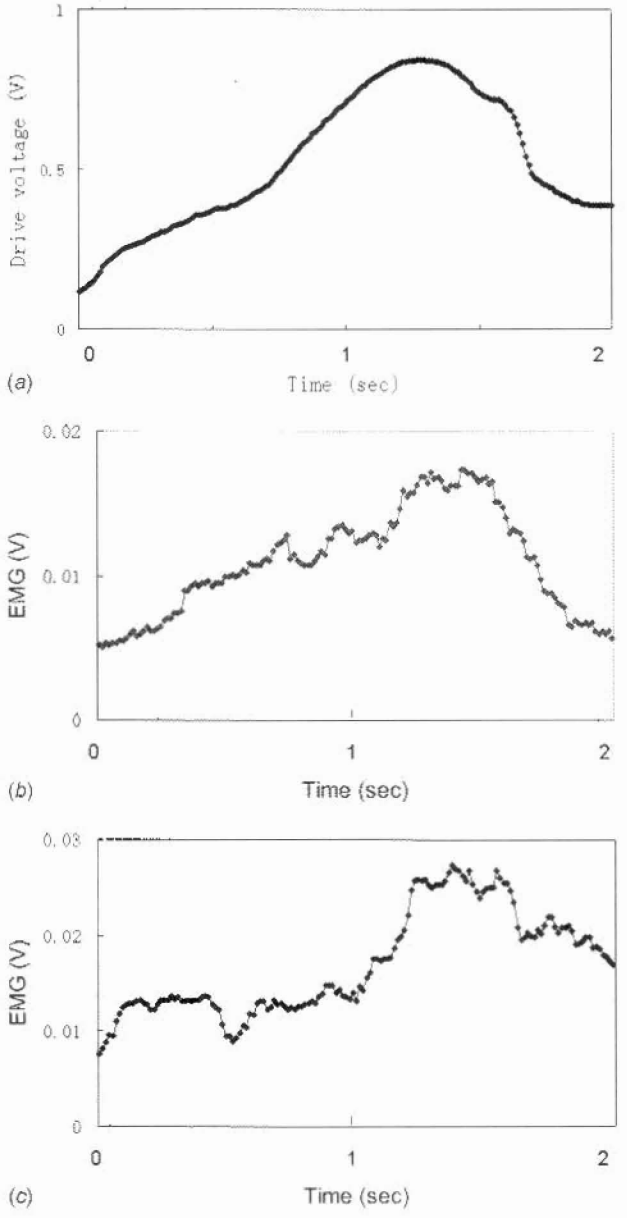

Fig. 19 (*a*) **Motor driven voltage,** (*b*) **EMG data of haptic interface, and** (*c*) **EMG data of actual action**

In addition, we need to consider another task look-up table for each joint jaw. We also need to consider an automatic acquisition method. For a complex task, there are a large number of muscles that must be used, and we need to consider what level of activation must be considered to realize the minimum construction of the force representation mechanism. Further, we need to consider the rotational tasks realized by multiple muscle activations, as in the wrist.

6 Conclusion

We developed a wearable exoskeleton haptic interface to fit the human body. In this study, the exoskeleton frame was fit to the joint jaw, and the joint jaw moment was generated. Multiple dc motors were used for representing the force at a number of moments. In addition, we developed a control system that included a motor controller, a data collection interface, and the control software.

A simple weight pull-up action experiment was used for the verification of the haptic interface. Appropriate force curves were generated from the EMG data. Experiments were evaluated by analyzing questionnaire results and comparing the EMG data between the haptic interface and the actual actions. From these experimental results, it was determined that the smoothed EMG curves could be used as force curves of the haptic interface for force representation.

In addition, we confirmed that the EMG data shapes provide force representation similar to the actual action under good conditions. The force curves for each joint are different for each individual.

In the future, we will try to use this haptic display in a real application. Rotation action, as in a wrist, will also be considered using our method.

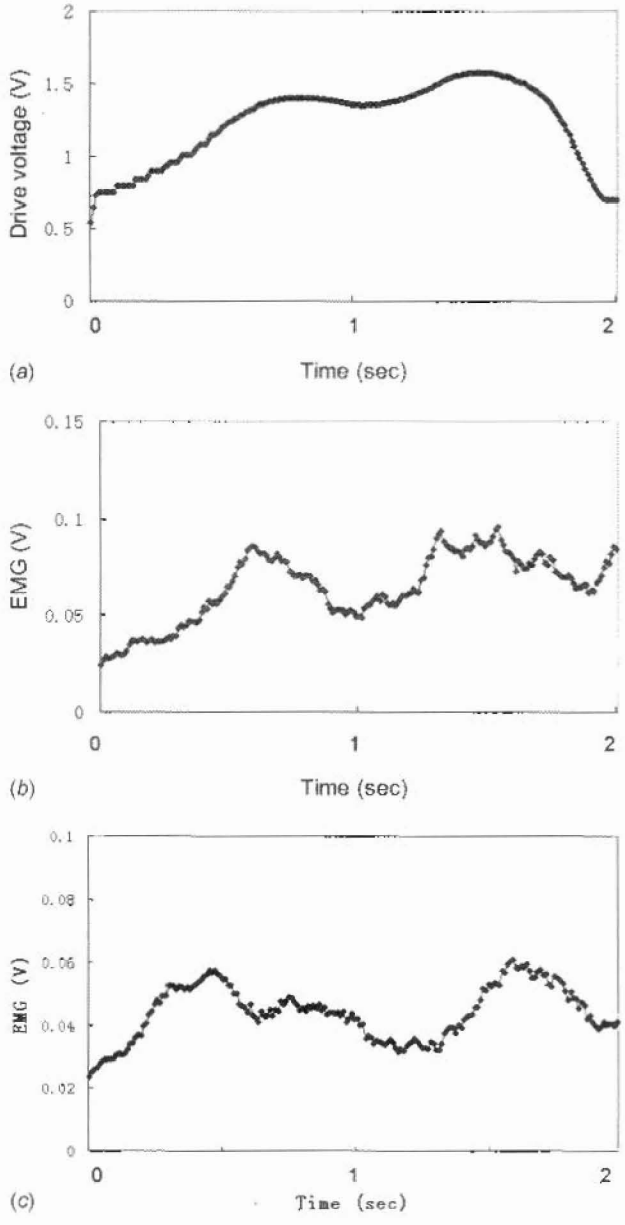

Fig. 20 (*a*) Motor driven voltage, (*b*) EMG data of haptic interface, and (*c*) EMG data of actual action

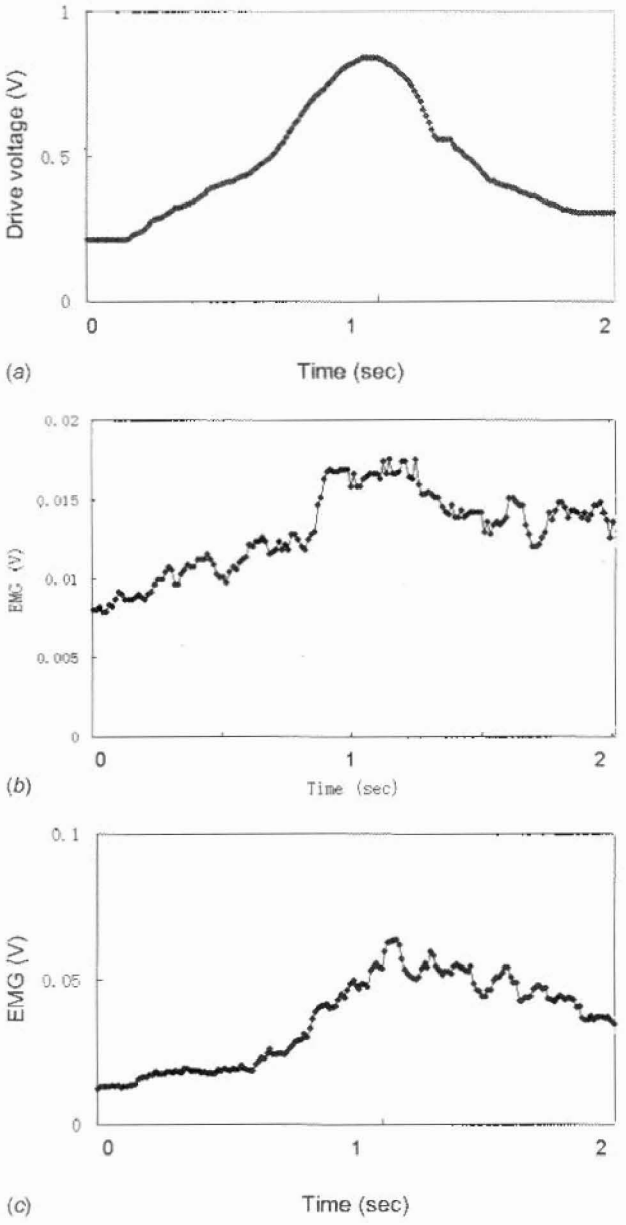

Fig. 21 Motor driven voltage, EMG data of haptic and actual action for palmaris longus and pattern 11, and lead time: 0 ms (subject C). (*a*) Motor driven voltage, (*b*) EMG data of haptic interface, and (*c*) EMG data of actual action.

Table 2 Correlation coefficient of the EMG data between haptic interface and the actual action for patterns 5 and 8

Pattern	CC of biceps brachii	CC of palmaris longus
5	0.82	0.57
8	0.64	0.82

References

[1] Burdea, G. C., 1996, *Force and Touch Feedback for Virtual Reality*, Wiley, New York.

[2] Massie, T., and Salisbury, J. K., 1994, *The Phantom Haptic Interface: A Device for Probing Virtual Objects, Proceedings of the Third Annual Symposium on Haptic Interfaces for Virtual Environment and Teleoperator Systems*, pp. 295–301.

[3] Sato, M., 2002, "Development of String-Based Force Display: SPIDAR," *Proceedings of the Eighth International Conference on Virtual Systems and Multi Media VSMM 2002*, pp. 1034–1039.

[4] Asano, T., Yano, H., and Iwata, H., 1996, "Basic Technology of Simulation System for Laparoscopic Surgery in Virtual Environment With Force Display," *Proceedings of the Virtual Reality Society of Japan Annual Conference*, pp. 95–98.

[5] Hirose, M., Ogi, T., and Yano, H., 1999, "Development of Wearable Force Display (HapticGEAR) for Immersive Projection Display," *Proceedings of the IEEE Virtual Reality Conference*.

[6] Tanaka Y., Sakai M., Kohno Y., Fukui Y., Yamashita J., and Nakamura N., 2001, "Mobile Torque Display and Haptic Characteristics of Human Palm," ICAT 2001.

[7] Ando, H., Obana, K., Watanabe, J., Sugimoto, M., and Maeda, T., 2003, "Development of a Rotation Moment-Type Force Display Using Mechanical Breaks," Journal of Human Interface Society, **5**(2), pp. 181–188.

[8] Amemiya, T., Ando, H., and Maeda, T., 2005, "Virtual Force Display: Direction Guidance Using Asymmetric Acceleration Via Periodic Translational Motion," *Proceedings of the IEEE World Haptics Conference 2005*, pp. 619–622.

[9] Iwata, H., and Nakagawa, H., 1998, "Wearable Force Feedback Joystick," Human Interface N&R, **13**(2), pp. 135–138.

[10] Maekawa, H., and Hollerbach, J., 1998, "Haptic Display for Object Grasping and Manipulating in Virtual Environment," *Proceedings of the 1998 IEEE International Conference on Robotics and Automation*, pp. 2566–2573.

[11] Gupta, A., and O'Malley, M., 2006, "Design of a Haptic Arm Exoskeleton for

Training and Rehabilitation," IEEE/ASME Trans. Mechatron., **11**(3), pp. 280–289.
[12] Kim, Y., Lee, J., Lee, S., and Kim, M., 2005, "A Force Reflected Exoskeleton-Type Masterarm for Human-Robot Interaction," IEEE Trans. Syst. Man Cybern., Part A. Syst. Humans, **35**(2), pp. 198–212.
[13] Sledd, A., and O'Malley, M., 2006, "Performance Enhancement of a Haptic Arm Exoskeleton," *Proceedings of the 2006 IEEE Symposium on Haptic Interfaces for Virtual Environment and Teleoperator Systems.*
[14] Kawamoto, H., Lee, S., Kanbe, S., and Sankai, Y., 2003, "Power Assist Method ForHAL-3 Using EMG-Based Feedback Controller," *Proceedings of the International Conference on Systems, Man, and Cybernetics (SMC2003)*, pp. 648–1653.
[15] Perry, J., and Rosen, J., 2006, "Design of a 7 Degree-of-Freedom Upper-Limb Powered Exoskeleton," IEEE/RAS-EMBS International Conference on Biomedical Robotics and Biomechatronics.
[16] Rosen, J., Fuchs, M., Arcan, M., 1999, "Performances of Hill-Type and Neural Network Muscle Models—Toward a Myosignal-Based Exoskeleton," Comput. Biomed. Res., **32**, pp. 415–439.
[17] Nishisaka, S., Ikeda, Y., and Fujita, K., 2006, "Haptic Broadcast: Remote Haptic Sharing of Elastic Objects Allowing Active Pinch Using Electromyogram for Force Estimation," Transaction of Virtual Reality Society of Japan, **11**(1), pp. 19–26.
[18] Kizuka, T., Masuda, T., Kiryu, T., and Sadoyama, T., 2006, *Practical Usage of Surface Electromyogram*, Tokyo Denki University Press.
[19] Osaki, R., Shimada, M., and Uehara, K., 1999, "Extraction of Primitive Motion for Human Motion Recognition," Lect. Notes Comput. Sci., **1721**, pp. 351–352.
[20] Liu, G., Zhang, J., Wang, W., and McMillan, L., 2005, "A System for Analyzing and Indexing Human-Motion Databases," *Proceedings of the 2005 ACM SIGMOD international Conference on Management of Data*, pp. 924–926.
[21] Kuchenbecker, K. J., Fiene, J., and Niemeyer, G., 2006, "Improving Contact Realism Through Event-Based Haptic Feedback," IEEE Trans. Vis. Comput. Graph., **12**(2), pp. 219–230.